Pharm Res (2020) 37:66
https://doi.org/10.1007/s11095-020-02789-w

RESEARCH PAPER

Design and Synthesis of Polymer Prodrugs for Improving Water-Solubility, Pharmacokinetic Behavior and Antitumor Efficacy of TXA9

Yiwen Li[1] • Chun Ye[1] • Chengcheng Cai[1] • Meng Zhao[1] • Na Han[1] • Zhihui Liu[1] • Jianxiu Zhai[1] • Jun Yin[1]

Received: 8 October 2019 / Accepted: 20 February 2020

ABSTRACT

Purpose TXA9, a novel cardiac glycoside, has a potent anti-proliferative effect against A549 human lung cancer cells, however, possesses a poor water-solubility and a rapid metabolic rate *in vivo* which limited the further development of TXA9. To overcome the shortcomings of TXA9, four polymer prodrugs of TXA9 were designed and synthesized.

Methods Poly (ethylene glycol) monomethyl ether (mPEG) and α-tocopherol polyethylene glycol succinate (TPGS) were applied to modify TXA9 via carbonate ester and glycine linkers respectively to obtain four polymer prodrugs. The water-solubility and stability of prodrugs were studied *in vitro* while their pharmacokinetic behaviors and antitumor activity were investigated *in vivo*.

Results The water-solubility of TXA9 was obviously increased and prodrugs with glycine linkers showed a better stability in rat plasma. Their pharmacokinetic investigation found that the $t_{1/2}$ and $AUC_{0-\infty}$ of TPGS-Gly-TXA9 was increased by 80- and 9.6-fold compared with that of TXA9, which was more superior than the other three prodrugs. More importantly, the tumor inhibition rate of TPGS-Gly-TXA9 (43.81%) on A549 xenograft nude mice was significantly increased compared with that of TXA9 (25.26%).

Conclusion The above results suggested that TPGS-Gly-TXA9 possessed better antitumor efficiency than TXA9 and could be further investigated as an anti-cancer agent.

Electronic supplementary material The online version of this article (https://doi.org/10.1007/s11095-020-02789-w) contains supplementary material, which is available to authorized users.

✉ Jun Yin
yinjun2002@yahoo.com

[1] School of Traditional Chinese Material, Shenyang Pharmaceutical University, Wenhua Road 103, Shenyang 110016, China

KEY WORDS antitumor activity · pharmacokinetics · polymer prodrug · TXA9 · water-solubility

ABBREVIATIONS

DCC	N, N'-dicyclohexylcarbodiimide
DMAP	4-Dimethylaminopyridine
EDCI	1-Ethyl-3-(3-dimethylaminopropyl) carbodiimide hydrochloride
EPR	Enhanced permeability and retention
mPEG	Poly (ethylene glycol) monomethyl ether
NSCLC	Non-small-cell lung cancer
PEG	Polyethylene glycol
pNPC	p-Nitrophenyl chloroformate
TPGS	α-Tocopherol polyethylene glycol succinate

INTRODUCTION

Non-small-cell lung cancer (NSCLC), a common subtype of lung cancer, is recognized as the most aggressive and life-threatening disease worldwide with a low 5-year overall survival rate (1,2). In our previous study, TXA9 (Fig. 1a), a novel cardiac glycoside separated from the roots of *Streptocaulon juventas* (Lour.) Merr., was found with a potent anti-proliferative effect on A549 human lung cancer cells through stimulating apoptosis via extrinsic pathway and cell cycle arrest in the SubG0/1 and G2/M periods (3,4). However, its poor water-solubility (0.15 mg/mL) and short half-life *in vivo* ($t_{1/2} < 5$ min) were found along with its good efficacy, which limited the further development of TXA9 as an anti-cancer agent.

Polyethylene glycol (PEG), the most widely applied carrier in chemical modification, could enhance water-solubility, prolong circulation time and achieve passive targeting via enhanced permeability and retention (EPR) effect of the

Published online: 12 March 2020

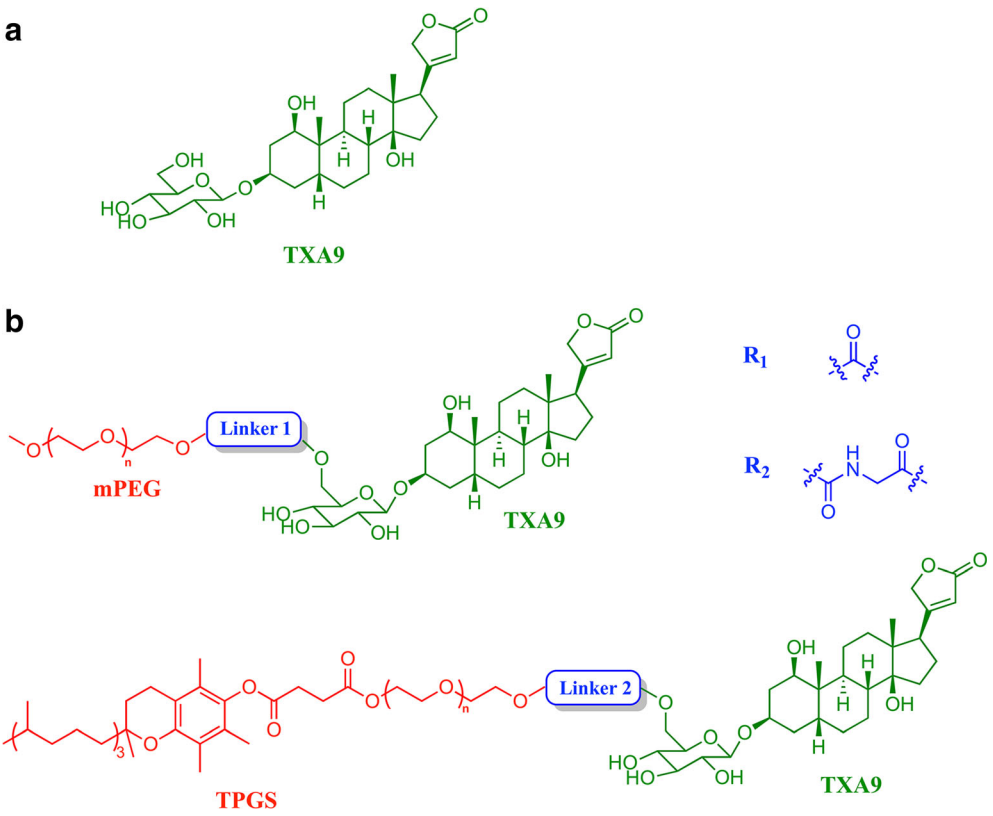

Fig. 1 (**a**) Structure of TXA9; (**b**) Structures of mPEG-p-TXA9 (Linker 1 = R_1), mPEG-Gly-TXA9 (Linker 1 = R_2), TPGS-p-TXA9 (Linker 2 = R_1) and TPGS-Gly-TXA9 (Linker 2 = R_2).

modified drug (5,6). α-Tocopherol polyethylene glycol succinate (TPGS) is a PEG derivative of α-tocopherol succinate, which has both advantages of PEG (hydrophilic group) and α-tocopherol (lipophilic group) for drug delivery, such as extending *in vivo* circulation time and enhancing the cellular uptake of drugs (7). Relative investigations had been reported that PEG and TPGS modification could significantly enhance the water-solubilities, prolong retention time *in vivo* and improve the antitumor efficacy of anti-cancer agent, such as paclitaxel (PTX), gambogic acid, doxorubicin, camptothecin and bufalin remarkably improved after the conjugation with PEG (8–16). Therefore, mPEG and TPGS were designed as drug carriers to be conjugated with TXA9 via carbonate ester and glycine linkers respectively aiming to improve the water-solubility, pharmacokinetic behavior and antitumor efficacy of TXA9.

In this study, four polymer prodrugs named mPEG-p-TXA9, mPEG-Gly-TXA9, TPGS-p-TXA9 and TPGS-Gly-TXA9 were synthesized (Fig. 1b) and characterized by ^{1}H-NMR, ^{13}C-NMR and FTIR. To compare the drug delivery capacities of prodrugs, the assessments of water-solubility and stability, assays for hemolysis and cytotoxicity (on A549 cells) were carried out *in vitro*, and pharmacokinetic study was conducted *in vivo*. In addition, the antitumor activity of TPGS-Gly-TXA9 on A549 xenograft nude mice was investigated due to its most superior pharmacokinetic property among four prodrugs.

MATERIALS & METHODS

Materials, Animals and Apparatus

TXA9 was isolated from the extract of the roots of *Streptocaulon juventas* as reported previously in our laboratory (3). Poly (ethylene glycol) monomethyl ether (mPEG, molecular weight (MW): 5 kDa) was purchased from Sigma Aldrich. Poly (ethylene glycol) (PEG, MW: 4 kDa) was purchased from Tianjin Kemiou Reagent Co., Ltd. Glycine and succinate anhydride (SA) were purchased from Tianjin Bodi Chemical Co., Ltd. α-Tocopherol, p-nitrophenyl chloroformate (pNPC), N, N'-dicyclohexylcarbodiimide (DCC), 4-dimethylaminopyridine (DMAP) and 1-ethyl-3-(3-dimethylaminopropyl) carbodiimide hydrochloride (EDCI) were purchased from Shanghai Darui Chemicals Co., Ltd. All chemicals used in this study were of HPLC grade.

Sprague-Dawley rats (180–220 g) (Certificate no. SCXK 2015–0001) and BALB/c-nude mice (18–20 g) (Certificate no. SCXK 2014–0004) were provided from the Experimental Center of Shenyang Pharmaceutical University. All experimental procedures were performed in accordance with the Institutional Animal Care and Use Ethics Committee of Shenyang Pharmaceutical University.

High Performance Liquid Chromatography (HPLC) was conducted by Agilent 1260 Infinity with DAD detector. Chromatographic column was ACCHROM Unitary C18

column (4.6 mm × 250 mm, 5 μm, 100A, P/N: 11190510525, S/N: 12021507). TXA9 and prodrugs was detected with a wavelength of 220 nm at 25°C.

Synthesis and Characterization of mPEG-p-TXA9, mPEG-Gly-TXA9, TPGS-p-TXA9 and TPGS-Gly-TXA9

Synthesis of mPEG-PNP

A dried round bottom flask was charged with mPEG (5.00 g, 1.00 mmol), pNPC (1.01 g, 5.00 mmol) and DMAP (0.24 g, 2.00 mmol) in anhydrous DCM (60 mL). After reacted with stirring at room temperature for 12 h, the mixture was washed by 10% citric acid solution and brine for three times respectively. The organic layer was dried over anhydrous Na_2SO_4, then filtered and concentrated in vacuum. The residue was purified by silica column chromatography (EtOAc: MeOH = 5:1 then DCM: MeOH = 8:1) to furnish mPEG-PNP (4.23 g, 82% yield).

Synthesis of mPEG-p-TXA9

mPEG-PNP (5.17 g, 1.00 mmol) was dehydrated by being refluxed in toluene (100 mL) for 2 h and then concentrated in vacuum, re-dissolved in anhydrous DCM (100 mL), after which, 4 mL anhydrous DMF containing TXA9 (0.83 g, 1.5 mmol) and DMAP (0.13 g, 1 mmol), were added dropwise. The reaction mixture was stirred at room temperature for 48 h and then washed by distilled water for three times to remove excess TXA9. The organic layer was washed by 10% citric acid solution and brine for three times respectively, dried over anhydrous Na_2SO_4, filtered and concentrated in vacuum. The residue was purified by dissolving it with a small amount of DCM and precipitating in excess cold diethyl ether, then the precipitate was filtered and dried to obtain the white powder (mPEG-p-TXA9, 3.32 g, 62% yield).

Synthesis of mPEG-Gly

To a solution of mPEG-PNP (4.00 g, 0.77 mmol) and glycine (0.44 g, 5.81 mmol) in acetonitrile/water (2/3, 60 mL), triethylamine (0.52 mL, 3.74 mmol) was added by dropwise. After stirred at room temperature for 5 h, the mixture was diluted with excess water and washed by diethyl ether for three times to remove the excess glycine. The water layer was extracted by DCM for five times to collect the organic layer. The organic layer was then washed with brine, dried over anhydrous Na_2SO_4, filtered and concentrated in vacuum. The residue was precipitated with diethyl ether as the method mentioned in the section of *synthesis of mPEG-p-TXA9* to afford mPEG-Gly (3.51 g, 89% yield).

Synthesis of mPEG-Gly-TXA9

mPEG-Gly (1.00 g, 0.20 mmol) and EDCI (0.08 g, 0.42 mmol) was dissolved in anhydrous DCM (30 mL) and stirred at 0°C for 30 min, after which, 1 mL anhydrous DMF, containing TXA9 (0.13 g, 0.24 mmol) and DMAP (0.02 g, 0.16 mmol), was added dropwise. After stirred at room temperature for 48 h, the mixture was treated with the same procedure as mentioned in the section of *synthesis of mPEG-p-TXA9* to obtain purified mPEG-Gly-TXA9 (0.99 g, 88% yield).

Synthesis of α-Tocopherol Succinate (α-TS)

SA (1.40 g, 13.99 mmol) was added to the solution of α-tocopherol (4.01 g, 9.31 mmol), DMAP (0.57 g, 4.67 mmol) and triethylamine (1.30 mL, 9.35 mmol) in anhydrous DCM (60 mL), and the mixture was stirred at room temperature for 2 h. The mixture was washed by 5% HCl solution and brine for three times respectively, dried over anhydrous Na_2SO_4, filtered and concentrated in vacuum. The residue was dissolved in 5.0 mL cold DCM, after which, the solution was filtered to remove excess SA and concentrated to provide **α-TS** (4.31 g, nearly 100% yield), which could be used without further purification.

Synthesis of TPGS

α-TS (0.79 g, 1.49 mmol) was reacted with PEG (3.82 g, 1.14 mmol) in the presence of DCC (0.31 g, 1.50 mmol) and DMAP (0.07 g, 0.57 mmol) in anhydrous DCM (50 mL) at room temperature for 24 h. The obtained product was filtered to remove N, N-dicyclohexylurea (DCU), washed by 5% HCl solution and brine for three times, dried over anhydrous Na_2SO_4, filtered and concentrated in vacuum. The residue was precipitated in cold diethyl ether overnight and the white precipitant was filtered to obtain TPGS (4.31 g, 87% yield).

Synthesis of TPGS-PNP and TPGS-Gly

The synthesis methods of TPGS-PNP and TPGS-Gly were identical with that of mPEG-PNP and mPEG-Gly except that mPEG and mPEG-PNP were substituted by TPGS and TPGS-PNP respectively. And the yields of TPGS-PNP and TPGS-Gly were 58% and 83% respectively.

Synthesis of TPGS-p-TXA9 and TPGS-Gly-TXA9

The synthesis procedures of TPGS-p-TXA9 and TPGS-Gly-TXA9 were the same with that of mPEG-p-TXA9 and mPEG-Gly-TXA9, however, TPGS-PNP and TPGS-Gly were used instead of mPEG-PNP and mPEG-Gly respectively. The yields of TPGS-p-TXA9 and TPGS-Gly-TXA9 were 77% and 71%.

Characterization of Prodrugs and Intermediates

The chemical structures of four prodrugs and their intermediates were confirmed by FTIR, ^{1}H-NMR and ^{13}C-NMR in $CDCl_3$ at 600 MHz. The purity of four prodrugs was evaluated by HPLC.

Determination of Drug Content

Drug contents of prodrugs were determined by ^{1}H-NMR. The ratio of integral values of characteristic proton signals of carriers and TXA9 was equal to the mole ratio of them and then drug content (wt%) could be indirectly calculated as Eq. 1 (for mPEG-p-TXA9 and mPEG-Gly-TXA9) and Eq. 2 (for TPGS-p-TXA9 and TPGS-Gly-TXA9) when the mole number of TXA9 was defined as 1. The double bond proton in unsaturated lactone ring was the characteristic proton signal of TXA9, and the special proton signals of carriers were the terminal methoxy proton for mPEG and the methyl proton on benzene ring for TPGS.

$$\text{Drug content (wt\%)} = M_{TXA9}/(M_{TXA9} + M_{mPEG} \times I_{mPEG}/I_{TXA9}/3) \times 100\% \quad (1)$$

$$\text{Drug content (wt\%)} = M_{TXA9}/(M_{TXA9} + M_{TPGS} \times I_{TPGS}/I_{TXA9}/3) \times 100\% \quad (2)$$

(M_{TXA9}, M_{mPEG} and M_{TPGS} were the molecular weights of TXA9, mPEG and TPGS respectively; I_{TXA9}, I_{mPEG} and I_{TPGS} were the absolute integral values of characteristic proton signals of TXA9, mPEG and TPGS in each ^{1}H-NMR spectrogram of prodrugs.)

Determination of Water-Solubility

Water-solubility of prodrugs was measured by a simple method of visual observation. In transparent test tubes, distilled water was added to dissolve a certain mass of prodrug powder (***m***, mg) by a diminutive volume of 5 μL each time. During the process of dissolution, the test tubes were shaken at 180 rpm in a 25°C water bath to ensure complete dissolution. When the prodrug solution was clarified without any powders, the volume of added water (***v***, mL) was recorded and the water-solubility was calculated as ***m/v***.

To determine water-solubility of TXA9, excess TXA9 were saturated in the quantificational distilled water and shaken at 180 rpm in a 25°C water bath for 24 h to achieve equilibration. The water-solubility of TXA9 was equal to the concentration of TXA9 in supernatant after centrifugation and measured by HPLC. The standard curve of TXA9 was established by HPLC ranging from 2 to 120 μg/mL with $r^2 = 0.9995$.

Characterization of TPGS Prodrug Micelles

The particle size, size distribution and zeta potential of the prodrug micelles were measured using Zetasizer (Nano ZS, Malvern Co., UK), and the measurements were repeated in triplicate. The morphology of the micelles was observed by transmission electron microscopy (TEM) (Hitachi, Japan). Samples were stained with 2% phosphotungstic acid.

Determination of Critical Micelle Concentration (CMC)

To determine the CMCs of TPGS and TPGS prodrugs, an UV spectroscopy method was used with iodine as the hydrophobic probe (17,18). The KI/I_2 standard solution was prepared by dissolving 6 mg of iodine and 12 mg of potassium iodide in 2 mL water. Thirteen samples of each prodrugs or TPGS with different concentration gradients ranging from 0.00391 mg/mL to 20 mg/mL were prepared. The mixtures of 110 μL of sample solution and 2 μL of KI/I_2 standard solution were added into 96-well plates and incubated for 24 h in the dark at 37°C in incubator shakers before measurement. The ultraviolet absorbance value of each sample was measured at 366 nm using a microplate reader. The absorbance was plotted against the logarithm of concentration, and CMC values corresponded to concentrations of prodrugs/carriers at which a sharp increase in absorbance was observed.

Stability Study of Prodrugs *In Vitro*

Stability Study of Prodrugs in Phosphate Buffered Solution (PBS)

Prodrugs were dissolved in 0.2 M PBS (pH = 5.0, 7.4 and 9.0 respectively) at a concentration of 0.1 mg/mL (***C***, equal to TXA9) and incubated at 37°C with gentle shaking. At designated time intervals of 0, 1, 2, 6, 8, 12, 24 h, 100 μL of PBS solution was collected and the concentrations of released TXA9 in collected PBS (C_x) were determined by HPLC, and the release rate was calculated as $C_x/C*100\%$ at each time point.

Stability Study of Prodrugs in Rat Plasma

1 mL of fresh plasma from Sprague–Dawley rats was preheated at 37°C for 5 min before prodrug was added to obtain a final concentration of 0.4 mg/mL (equal to TXA9) for each sample, which was kept at 37°C with shaking at 180 rpm. 100 μL of samples was taken up at designated time intervals of 0, 1, 2, 6, 8, 12, 24 h, and mixed and vortexed for 1 min with 500 μL of methanol to precipitate proteins. After a centrifugation of 12,000 rpm for 10 min, the concentrations of released TXA9 in sample and the release rates were determined with the similar method as mentioned in ***Stability study of prodrugs in phosphate buffered solution (PBS)***.

Hemolysis Assay

Hemolysis assay was performed to evaluate the biocompatibility of prodrugs as the method reported (19). Briefly, red blood cells (RBC) were isolated from 10 mL defibrinated rabbit blood by centrifugation (2500 rpm for 10 min at 4°C), and then resuspended with saline to obtain 2.0% (*v*/v) suspension. A series of 2.5 mL prodrug solutions in saline with different concentrations ranging from 0.1 to 0.5 mg/mL (equal to TXA9) were mixed with 2.5 mL of the prepared RBC suspension prior to an incubation for 3 h at 37°C in water bath. Meanwhile, 2.5 mL RBC suspension was dispersed in 2.5 mL saline or 2.5 mL distilled water to serve as negative or positive control respectively. Subsequently, all tested solutions were centrifugated at 2500 rpm for 10 min to separate damaged erythrocytes and their membranes, and the absorbance of supernatant was determined at 545 nm by ultraviolet spectrophotometer to calculate the hemolytic rate as Eq. 3.

$$\text{Hemolytic rate}\ (\%) = (A_s - A_0)/(A_p - A_0) \times 100\% \quad (3)$$

(A_s, A_0 and A_p were the absorbance of samples, negative control and positive control respectively.)

In Vitro Cytotoxicity

A549 cells were seeded in a 96 − well culture plate at 5×10^3 cells/well and after an incubation of 24 h at 37°C with 5% CO_2, medium was replaced by 200 μL of DMEM supplemented with 10% fetal bovine serum containing different concentrations of cisplatin, TXA9 or four prodrugs for an incubation of 48 h. Cell viability was measured using MTT assay standard protocol and the values of IC_{50} were calculated by GraphPad PRISM.

Pharmacokinetic Study

Sprague–Dawley rats (200–250 g) were utilized to investigate the pharmacokinetics of four prodrugs. All animals were fasted over night with free access to water and randomly divided into 5 groups (6 rats for each group). After an intravenous administration of TXA9, mPEG-p-TXA9, mPEG-Gly-TXA9, TPGS-p-TXA9 and TPGS-Gly-TXA9 at a dose of 5 mg/kg equivalent to TXA9 respectively, blood samples were collected into EP tubes at 5, 15, 30, 45, 60, 90, 120 and 180 min. After a centrifugation of 6000 rpm for 10 min, plasma samples were precipitated protein with methanol and centrifugated at 12000 rpm for 10 min to obtain the supernatants, in which the concentrations of TXA9 were measured by HPLC. The validation of analytical method was performed using blank rat plasma and the internal standard was icariin. Pharmacokinetic parameters were calculated with DAS 2.0. software (Mathematical Pharmacology Professional Committee of China, Shanghai, China) by non-compartment analysis.

In Vivo Antitumor Activity Study

30 BALB/c-nude mice were subcutaneously injected 3×10^6 A549 cells/mice into right flank. When average tumor volume of mice reached to 100 mm^3 (tumor volume = length × $width^2/2$, measured with a vernier caliper), mice were divided into 5 groups (6 mice for each group). The mice were injected intravenously with saline (control group), cisplatin (4 mg/kg), TXA9 (5 mg/kg), TPGS-Gly-TXA9 (5 and 10 mg/kg equivalent to TXA9) respectively 3 times a week for four weeks. Tumor volumes and body weights of mice were monitored every 2 days. After treatment for 28 days, serum samples were collected, and mice were sacrificed by cervical vertebra dislocation followed by separation of tumor tissues and organs (heart, liver, spleen, lung, kidney) to be weighted. The serum samples were used to measure the biochemical indexes (aspartate aminotransferase (AST), alanine aminotransferase (ALT), alkaline phosphatase (ALP), lactic dehydrogenase (LDH), blood urea nitrogen (BUN), creatinine (Crea), and total protein (TP)) by using standard reagent kits and microplate reader. Tumor inhibition rate (TIR) and organ indices were calculated as Eq. 4 and 5.

$$\text{TIR}(\%) = (1 - W_{\text{treated}}/W_{\text{control}}) \times 100\% \quad (4)$$

($\boldsymbol{W_{control}}$ and $\boldsymbol{W_{treated}}$ were the weights of tumor tissues of control group and treated groups.)

$$\text{Organ indices}\ (\text{mg/g}) = m_1/m_2 \quad (5)$$

($\boldsymbol{m_1}$ and $\boldsymbol{m_2}$ were the organ weights and body weights of mice.)

Statistical Analysis

Data were expressed as the mean ± standard deviation of at least three replicates. Statistical comparisons were performed using analysis of variance (ANOVA) (t-tests). All statistical computations were performed using SPSS (version 21.0).

RESULTS

Synthesis and Characterization of mPEG-p-TXA9, mPEG-Gly-TXA9, TPGS-p-TXA9 and TPGS-Gly-TXA9

Synthesis route of four prodrugs was outlined as Fig. 2. To synthesis mPEG-p-TXA9 and TPGS-p-TXA9, mPEG and TPGS reacted with pNPC to form activated ester (mPEG-PNP and TPGS-PNP) firstly, and then they reacted with TXA9 by transesterification. On the other hand, after

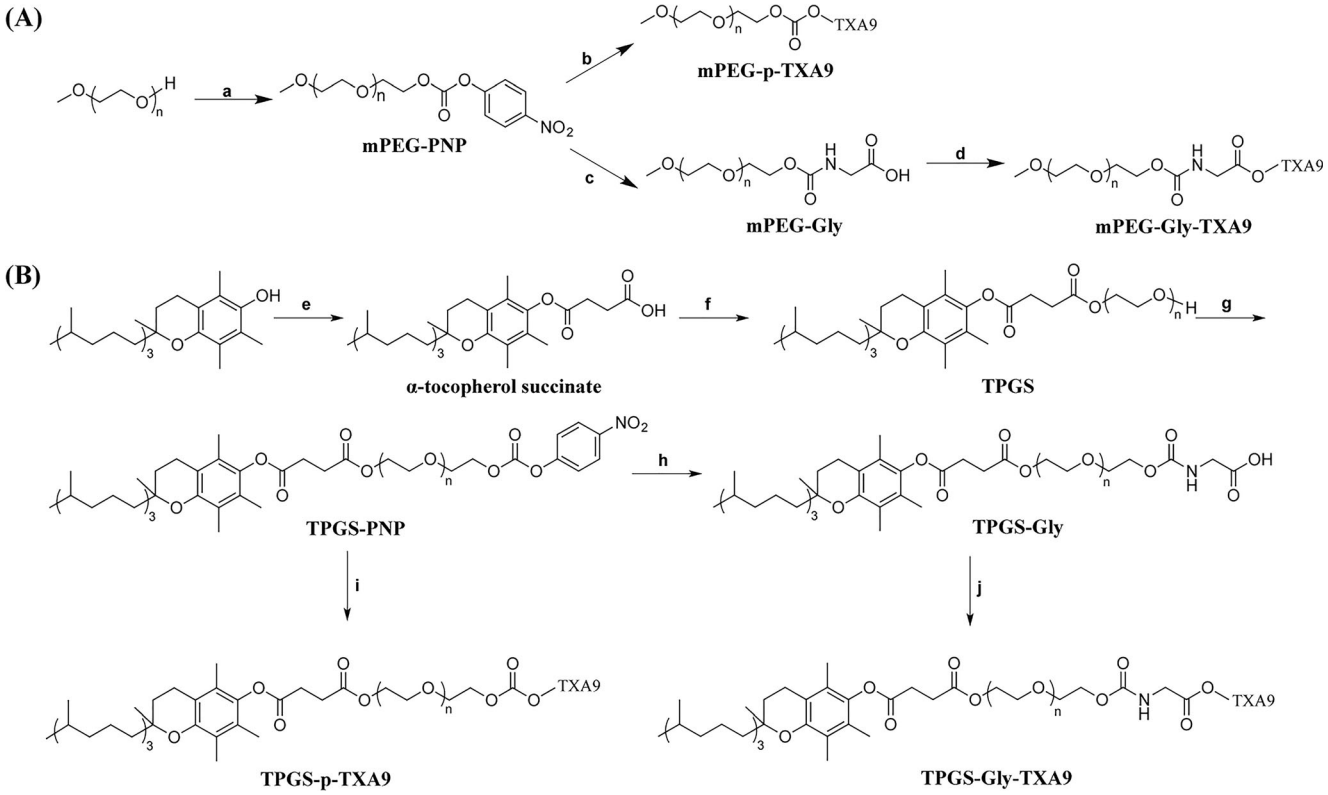

Fig. 2 (**A**) The synthesis route of mPEG-p-TXA9 and mPEG-Gly-TXA9. Reagents and conditions: (*a*) pNPC and DMAP in anhydrous DCM; (*b*) TXA9 and DMAP in anhydrous DMF and anhydrous DCM; (*c*) Gly and TEA in acetonitrile/H_2O (2/3); (d) EDCI, TXA9 and DMAP in anhydrous DMF and anhydrous DCM; (**B**) The synthesis route of TPGS-p-TXA9 and TPGS-Gly-TXA9. Reagents and conditions: (e) succinic anhydride, DMAP and TEA in anhydrous DCM; (*f*) PEG_{4k}, DCC and DMAP in anhydrous DCM; (*g*) pNPC and DMAP in anhydrous DCM; (*h*) Gly and TEA in acetonitrile/H_2O (2/3); (*i*) TXA9 and DMAP in anhydrous DMF and anhydrous DCM; (*j*) EDCI, TXA9 and DMAP in anhydrous DMF and anhydrous DCM.

mPEG-PNP or TPGS-PNP reacted with glycine to form carbamate, mPEG-Gly-TXA9 or TPGS-Gly-TXA9 was synthesized by esterification reaction between mPEG-Gly/TPGS-Gly and TXA9 in the presence of DMAP and EDCI.

The structures of prodrugs and intermediates were confirmed by ^{1}H-NMR, ^{13}C-NMR and FTIR. The related spectra were shown as Figure S1-S22. The ^{1}H-NMR spectra of prodrugs (Figure S7-S10) contained signals of TXA9 and carriers exhibiting typical peaks at 5.88, 4.99, 4.81 ppm which belonging to the protons of unsaturated lactone ring in TXA9, and peaks at 3.65 ppm which belonging to methylene protons of polyethylene oxide part in carriers. Compared with the peaks at 3.86, 3.68 ppm in the spectrum of TXA9 (Figure S11) which belonging to the methylene protons in glucose, these characteristic proton signals increased to 4.04 and 3.88 ppm in the spectra of four prodrugs, indicating that carriers had been conjugated with TXA9 by forming ester bond. In addition, for mPEG-p-TXA9 and TPGS-p-TXA9, the peaks at 4.45 ppm belonging to the methylene protons of mPEG, which was adjacent to TXA9, split into several peaks compared with that in the spectra of mPEG-PNP and TPGS-PNP (Figure S1 and Figure S5) due to the influence of TXA9. Similarly, the peaks of the methylene protons of glycine in the spectra of mPEG-Gly-TXA9 and TPGS-Gly-TXA9 also split into several peaks and their chemical shift increased from 3.11 in the spectra of mPEG-Gly and TPGS-Gly (Figure S2 and Figure S6) to 4.31. These confirmed the conjugation of four prodrugs.

For ^{13}C-NMR spectra of prodrugs (Figure S18-S21), the characteristic carbon signals of unsaturated lactone ring and glucose in TXA9 were at 174.54, 174.32, 117.32 ppm and 61.55 (C-6'), 101.17 ppm (C-1') respectively. In the spectra of mPEG-p-TXA9 and mPEG-Gly-TXA9, the peaks at 58.93 and 70.46 ppm belonged to the characteristic carbon signals of mPEG. For TPGS-p-TXA9 and TPGS-Gly-TXA9, the peaks at 149.45, 140.47, 126.71, 124.97, 123.03, 117.40 ppm and 172.23, 170.97 ppm were the carbon signals of benzene ring and carbonyl groups of succinic anhydride linker. Moreover, the peak at 152.36 ppm in the spectrum of mPEG-p-TXA9 and the peak at 155.79 ppm in the spectrum of TPGS-p-TXA9 belonged to the carbonyl carbon signals of carbonate ester linker. For glycine linker, the carbonyl carbon signals of carbamate and carboxylate ester were at 170.12/170.11 and 156.50/155.79 ppm in the spectra of for mPEG-Gly-TXA9 and TPGS-Gly-TXA9 respectively. These results proved the successful conjugation between TXA9 and carriers.

For the FTIR spectra of prodrugs and intermediates (Figure S22), the C-H and C-O stretching vibration ($\nu_{C\text{-}H}$ and $\nu_{C\text{-}H}$) of PEG showed the peaks at 2888 and 1113 cm^{-1}, which were the typical signals of mPEG and TPGS. The peak at 1631 cm^{-1} stood for the C=O stretching vibration ($\nu_{C=O}$) of carbamate in mPEG-Gly, but the adsorption of this peak increased because of the $\nu_{C=O}$ of the unsaturated lactone ring of TXA9 in mPEG-Gly-TXA9. For mPEG-PNP, the peak at 1631 cm^{-1} presented the C=C stretching vibration ($\nu_{C=C}$) of benzene ring. However, the adsorption of this peak decreased due to the departure of nitrobenzene ring and the import of the unsaturated lactone ring of TXA9 in mPEG-Gly-TXA9. For TPGS prodrug, the above changes at 1631 cm^{-1} were not appeared due to the disturbance of the $\nu_{C=C}$ of benzene ring in TPGS. After conjugated with TXA9, the C=O adsorption peak of carbonate ester in mPEG-PNP (1764 cm^{-1})/TPGS-PNP (1765 cm^{-1}) shifted to 1735/1751 cm^{-1} in mPEG-p-TXA9/TPGS-p-TXA9 due to the conjugation with TXA9. Similarly, the C=O adsorption peak of carboxylic acid in mPEG-Gly (1721 cm^{-1})/TPGS-Gly (1737 cm^{-1}) also shifted to 1735/1751 cm^{-1} in mPEG-Gly-TXA9/TPGS-Gly-TXA9. These further implied the successful conjugation of four prodrugs.

The purity of mPEG-p-TXA9, mPEG-Gly-TXA9, TPGS-p-TXA9 and TPGS-Gly-TXA9 was 95.2%, 97.5%, 98.4% and 99.1% respectively, and their HPLC diagrams were shown as Figure S23.

Determination of Drug Content

As shown in Table I, the drug contents of mPEG-p-TXA9, mPEG-Gly-TXA9, TPGS-p-TXA9 and TPGS-Gly-TXA9 were 5.40, 6.95, 3.26 and 5.47 wt% respectively. Drug contents of prodrugs with glycine linker (mPEG-Gly-TXA9 and TPGS-Gly-TXA9) were higher than that of prodrugs with carbonate ester linker (mPEG-p-TXA9 and TPGS-p-TXA9). The reason of this result could be explained that the reaction efficiency of esterification reaction was stronger than that of transesterification when polymer carriers were conjugated with TXA9. On the other hand, the drug contents of mPEG prodrugs were obviously higher than that of TPGS prodrugs, indicating the conjugation of mPEG intermediates to TXA9 was easier than that of TPGS intermediates. This might be probably due to the formation of intermolecular hydrogen bond between carbonyl group of ester bond in TPGS and hydroxyl group of glucose in TXA9 (20), which was a weak resistance for the hydroxyl group of TXA9 to attack the carbonyl carbon to accomplish the esterification or transesterification.

Table I The Absolute Integral Values of Characteristic Proton Signals and Drug Contents of mPEG-p-TXA9, mPEG-Gly-TXA9, TPGS-p-TXA9 and TPGS-Gly-TXA9

	I_{TXA9}*	I_{mPEG}*	I_{TPGS}*	Drug content (wt%)
mPEG-p-TXA9	672.69	3880.90	–	5.40
mPEG-Gly-TXA9	903.28	3938.67	–	6.95
TPGS-p-TXA9	850.32	–	9403.94	3.26
TPGS-Gly-TXA9	820.28	–	5220.00	5.47

* I_{TXA9}, I_{mPEG} and I_{TPGS} were the absolute integral values of characteristic proton signals of TXA9 (the double bond proton of unsaturated lactone ring), mPEG (the terminal methoxy proton) and TPGS (the methyl proton of benzene ring) in each ^{1}H-NMR spectrogram of prodrugs

Determination of Water-Solubility

The addition of co-solvent was found to be necessary during the administration of TXA9 due to its poor water-solubility, which on the other side, could lead to vascular irritations and the other side effects. To avoid this dilemma, four prodrugs of TXA9 was synthesized and their water-solubility were investigated. As shown in Table II, mPEG-p-TXA9, mPEG-Gly-TXA9, TPGS-p-TXA9 and TPGS-Gly-TXA9 increased the water-solubility of TXA9 from 0.15 mg/mL to 22.84, 31.06, 1.48 and 2.87 mg/mL, which were 152, 207, 10 and 19 folds respectively.

Characterization and CMC Determination of TPGS Prodrug Micelles

For TPGS prodrugs, the amphiphilic structure of TPGS promoted prodrugs to self-assemble into micelles after dissolved into water. Thus, the size, zeta potential and morphology of TPGS prodrug micelles were investigated. As shown in Figure S24, the size of TPGS prodrugs were 29.51 ± 0.59 nm and 21.42 ± 1.24 nm, which had no obvious differences with that of TPGS (26.48 ± 0.75 nm). However, their zeta potentials (−1.08 ± 0.16 mV for TPGS-p-TXA9 and 2.51 ± 0.70 mV for TPGS-Gly-TXA9) were higher than that of TPGS (−7.43 ± 0.69 mV), indicating that TXA9 might affect the surface charge of micelles and the increased zeta potential might be attributed to the weak positive

Table II Water-Solubility of Prodrugs and the Multiple of the Increased Water-Solubility of each Prodrug Compared with that of TXA9

Drug	Water-solubility (mg/mL, eq. TXA9)	Multiple*
TXA9	0.15 ± 0.00	–
mPEG-p-TXA9	22.84 ± 0.58	152
mPEG-Gly-TXA9	31.06 ± 0.42	207
TPGS-p-TXA9	1.48 ± 0.01	10
TPGS-Gly-TXA9	2.87 ± 0.02	19

Each value represented as the mean ± SD ($n = 3$)

* Multiple was the ratio of the water-solubility values of each prodrug and TXA9

electricity of TXA9 and glycine linker. The TEM images showed that the morphology of micelles was generally spherical as reported (21).

The CMC of prodrugs were increased to 3.47 mg/mL for TPGS-p-TXA9 and 3.23 mg/mL for TPGS-Gly-TXA9 compared with that of TPGS (1.45 mg/mL), indicating that the conjugation of TXA9 limited TPGS to form micelles to some extent because of the poor hydrophobicity of TXA9. Besides, there was no obvious difference between two TPGS prodrugs, illustrating that the linkers didn't affect the formation of micelles.

Stability Study of Prodrugs *In Vitro*

The stability of prodrugs and the representative HPLC diagrams were exhibited in Fig. 3 and Figure S25. As shown in Fig. 3, all prodrugs exhibited a quick release during the first 8 h and a slow release during the following period until 24 h. The drug release from the prodrugs with glycine linkers were obvious higher than that from the prodrugs with carbonate ester bond linkers in PBS at different pH value. At 24 h, the TXA9 release rate from mPEG-p-TXA9, mPEG-Gly-TXA9, TPGS-p-TXA9 and TPGS-Gly-TXA9 were 2.9%, 10.8%, 1.4% and 8.6% at pH 5.0, which increased to 17.4%, 40.5%, 14.7% and 28.4% at pH 7.4 and 51.1%, 80.0%, 37.8% and 86.0% at pH 9.0, indicating that TXA9 was prone to release from prodrugs at pH = 7.4 or 9.0 and difficult to release at pH = 5.0.

However, in rat plasma (Fig. 3d), the final release of prodrugs with carbonate ester linker increased dramatically compared with that in pH 7.4 PBS because of the influence of plasma enzymes, reaching to 86.0% for mPEG-p-TXA9 and 76.7% for TPGS-p-TXA9. On the contrary, the TXA9 release from mPEG-Gly-TXA9 and TPGS-Gly-TXA9, which was conjugated with glycine linkers, were only 48.1% and 38.4% in rat plasma, indicating a well stability of glycine linkers in rat plasma.

Hemolysis Assay

Hemolysis assay was carried out to assess the feasibility of intravenous administration of prodrugs. As shown in Fig. 4, the hemolytic rates of four prodrugs at the studied concentrations were less than 5% which was defined as non-hemolysis (19), implying the biocompatibility and security of prodrugs for intravenous injection.

In Vitro Cytotoxicity

A549 cells were employed to evaluate the *in vitro* cytotoxicity of prodrugs via MTT assay. As shown in Table III, TXA9 (IC_{50} = 0.072 μM) showed a stronger cytotoxicity than positive control cisplatin (IC_{50} = 18.04 μM). The IC_{50} values of mPEG-p-TXA9, mPEG-Gly-TXA9, TPGS-p-TXA9 and TPGS-Gly-TXA9 were 0.154, 0.121, 0.126 and 0.092 μM respectively. Although the activities of prodrugs were weaker than that of TXA9 to some extent, prodrugs exhibited the desirable cytotoxicity as well. From the comparison between prodrugs with the same carrier, prodrugs with glycine linker had the stronger cytotoxicity than prodrugs with carbonate ester linker. On the other hand, TPGS-p-TXA9/TPGS-Gly-TXA9 exhibited the more powerful inhibition on A549

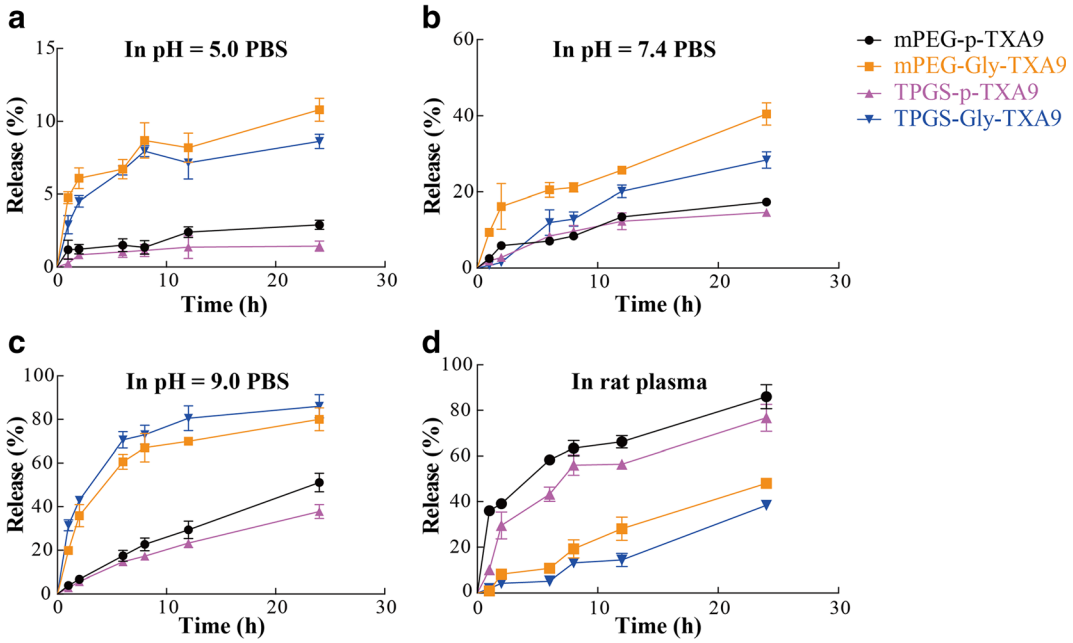

Fig. 3 Stability study of prodrugs *in vitro*. TXA9 release profiles from mPEG-p-TXA9, mPEG-Gly-TXA9, TPGS-p-TXA9 and TPGS-Gly-TXA9 in PBS at pH = 5.0 (**a**), pH = 7.4 (**b**), pH = 9.0 (**c**) and in rat plasma (**d**) at 37°C. Each value represented as the mean ± SD (n = 3).

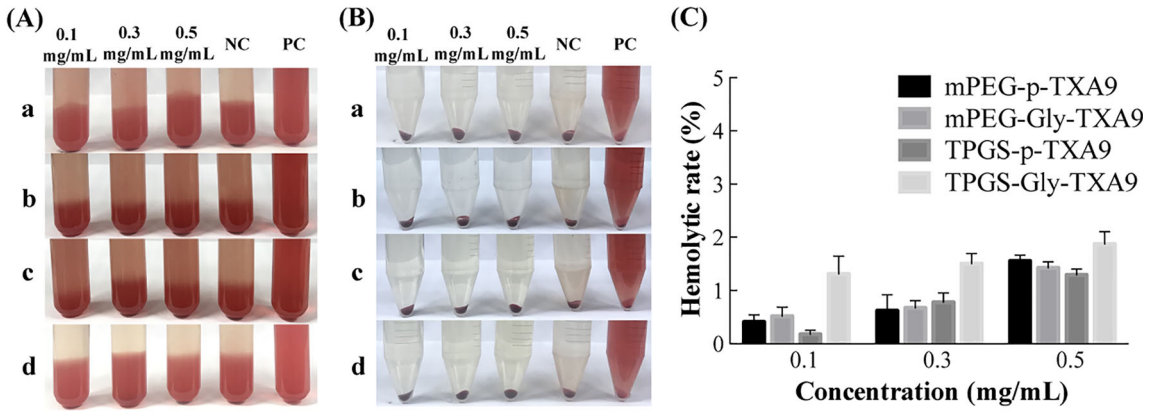

Fig. 4 Hemolysis assay was conducted with 2% (*v/v*) red blood cells suspension isolated from rabbit blood. (**A**-**B**) Images of the tested solutions of (*a*) mPEG-p-TXA9, (*b*) mPEG-Gly-TXA9, (*c*) TPGS-p-TXA9 and (*d*) TPGS-Gly-TXA9 at different concentrations (0.1, 0.3 and 0.5 mg/mL equal to TXA9) before (**A**) and after (**B**) centrifugation. Saline and distilled water were used as negative control (NC) and positive control (PC) respectively; (**C**) Hemolytic rate of four prodrugs at different concentrations equal to TXA9. Each value represented as the mean ± SD (n = 3).

cells compared with mPEG-p-TXA9/mPEG-Gly-TXA9, illustrating that TPGS was beneficial to increase the inhibitory activity of prodrugs.

Pharmacokinetic Study

The concentration-time profiles of TXA9 in plasma were determined after single intravenous administrations of TXA9 and prodrugs at 5 mg/kg TXA9 equivalency, which were shown in Fig. 5. The representative HPLC diagram and the results of the validation of analytical method were shown in Figure S26–27 and Table S1, indicating well specificity, precision, accuracy and extract recovery. The free TXA9 rapidly disappeared from circulation due to its short half-life *in vivo*. However, four prodrugs were found with longer circulation time to different extent compared with that of TXA9, which was mentioned as enhancing the half-life *in vivo*. The plasma concentration of TPGS-Gly-TXA9 group declined more slowly than the other three prodrugs, indicating its potential improved antitumor efficacy.

The pharmacokinetic parameters were calculated using non-compartmental model and shown in Table IV. Compared with free TXA9, prodrugs exhibited the longer half-life ($t_{1/2}$) and mean residence time (MRT), a slower clearance (CL) and a higher AUC respectively, confirming the improved pharmacokinetic property of TXA9 after conjugated with polymer carriers. Among four prodrugs, mPEG-Gly-TXA9 and TPGS-Gly-TXA9, which conjugated with glycine linkers, showed 8.2 and 6.7 times longer $t_{1/2}$ than mPEG-p-TXA9 and TPGS-p-TXA9, which conjugated with carbonate ester linkers respectively, indicating glycine linker was more stable than carbonate ester linker *in vivo*. This was similar to the previous report that amide bond, which was formed via amino acids, was more stable than ester bond to chemical and enzymatic hydrolysis (22). Compared with mPEG-Gly-TXA9, TPGS-Gly-TXA9 improved the pharmacokinetic property by prolonging $t_{1/2}$ and MRT by 1.5 and 2.5 folds, decreasing CL by 2.5 folds and thus increased the AUC by 2.6 folds, which demonstrated a better slow-release effect *in vivo*.

Table III The IC_{50} Values of Cisplatin, TXA9 and Prodrugs (eq. TXA9) on A549 Cells for 48 h

Substance	IC_{50} (μM)
Cisplatin	18.043 ± 2.162
TXA9	0.072 ± 0.007
mPEG-p-TXA9	0.154 ± 0.024
mPEG-Gly-TXA9	0.121 ± 0.023
TPGS-p-TXA9	0.126 ± 0.019
TPGS-Gly-TXA9	0.092 ± 0.014

Each value represented as the mean ± SD ($n = 3$)

In Vivo Antitumor Activity Study

Tumor volume–time curves were illustrated in Fig. 6a. Compared with control group, TXA9 and TPGS-Gly-TXA9 could inhibit the tumor growth to various extent after the treatment of 28 days. The tumor volume of low dose group of TPGS-Gly-TXA9 was 578.82 ± 64.93 mm^3 on day 28, which was markedly smaller than that of TXA9 group (760.09 ± 198.49 mm^3) at the same equivalent dose, indicating the improved antitumor efficacy of it. Images of the tumor tissues excised after the treatment were showed in Fig. 6b, and the tumor inhibition rates (TIRs) were calculated based on the weights of tumor tissues (Fig. 6c). The TIR of TPGS-Gly-TXA9 group (5 mg/kg) was found to be 43.81%, which was much improved antitumor efficacy compared with that of free TXA9 group (25.26%). To our delighted, the tumor inhibition rate of TPGS-Gly-TXA9 at a dose of 10 mg/kg (52.46%) had little difference with

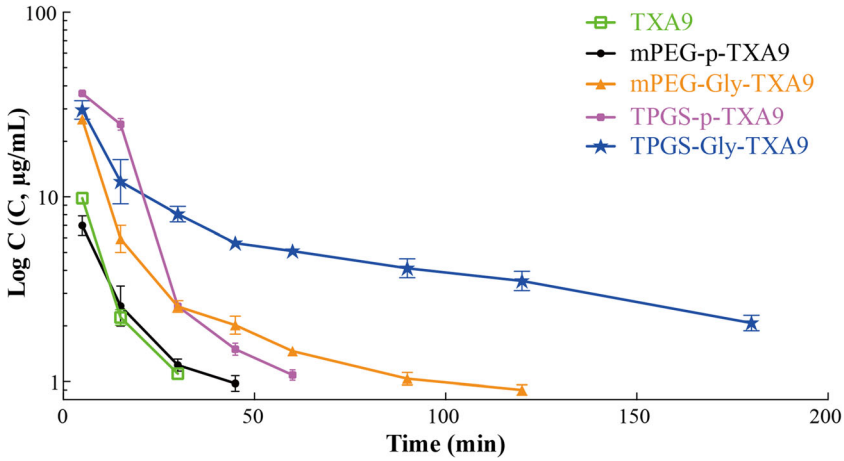

Fig. 5 Concentration-time profiles of TXA9 in plasma after an intravenous injection of TXA9, mPEG-p-TXA9, mPEG-Gly-TXA9, TPGS-p-TXA9 and TPGS-Gly-TXA9 to Sprague–Dawley rats (6 rats for each group) at a dose of 5 mg/kg equal to TXA9. Each value represented as the mean ± SD ($n = 6$).

that of positive control – cisplatin (54.57%), demonstrating the potential antitumor efficacy of TPGS-Gly-TXA9.

During the treatment, body weights and organ indexes of TXA9 and TPGS-Gly-TXA9 groups showed no significant difference compared with that of control group, demonstrating no systemic toxicity of free TXA9 and TPGS-Gly-TXA9 *in vivo* (Fig. 7a-b). For cisplatin group, the body weight (the increased body weight after day 19 was attributed to the death of two mice with serious body weight lost and side effects.) and organ indexes of liver, spleen and kidney decreased significantly compared with that of control group, indicating the toxicity of cisplatin as reported previously. In addition, the serum biochemical indexes (Table S2) and H&E staining analysis of organs (Fig. 7c) of TPGS-Gly-TXA9 group at a dose of 10 mg/kg did not exhibited any difference compared with that of control group, confirming the systemic safety of TPGS-Gly-TXA9 furthermore.

DISCUSSION

In this study, to improve the water-solubility, pharmacokinetic behavior and antitumor efficacy of TXA9, mPEG and TPGS were applied to modify TXA9 via carbonate ester and glycine linkers respectively to obtain four polymer prodrugs. It was reported that moderate molecular weight PEG exhibited better antitumor effects, although it should reach at least 20 kDa to avoid rapid elimination through urine (23). For example, PEG with a molecular weight of 8000 showed the greatest inhibition to colon cancer among a wide range of PEG species (400–35,000 Da) (24). Similarly, $mPEG_{5k}$-GFLF-doxorubicin displayed the highest antitumor activity in rats than the other conjugates with molecular weights of PEG ranging from 5 to 20 kDa (25). What's more, the drug content of prodrugs would inevitably decrease with the molecular weight of PEG increasing. Thus, taking both cytotoxicity and pharmacokinetics into consideration, commercially available mPEG (MW: 5 kDa) and PEG (MW: 4 kDa) were selected in this study, aiming to ensure the similar molecular weight of drug carriers. The successful synthesis of four prodrugs was confirmed by FTIR, ^{1}H-NMR and ^{13}C-NMR.

Then drug contents were indirectly obtained from the ^{1}H-NMR spectra. It was reported that the drug content of polymer prodrugs has been usually determined by using UV-Vis spectroscopy based on standard curve (26). In our study, the maximum absorption wavelength of TXA9 was at 220 nm and TPGS also had strong absorption at the same wavelength. Thus, the UV-Vis spectroscopy couldn't be used to measure the content of TXA9 precisely. Here, we obtained the accurate drug contents indirectly from the ratio of absolute integral

Table IV Pharmacokinetic Parameters of TXA9, mPEG-p-TXA9, mPEG-Gly-TXA9, TPGS-p-TXA9 and TPGS-Gly-TXA9 After an Intravenous Dose of 5 mg/kg Equal to TXA9

	TXA9	mPEG-p-TXA9	mPEG-Gly-TXA9	TPGS-p-TXA9	TPGS-Gly-TXA9
C_{max} (mg/L)	9.83 ± 0.09	6.99 ± 0.91*	26.36 ± 1.43***	36.41 ± 1.35***	29.62 ± 3.61***
$t_{1/2}$ (h)	0.02 ± 0.00	0.13 ± 0.08	1.07 ± 0.51***	0.24 ± 0.10*	1.60 ± 0.22***
$MRT_{0-\infty}$ (h)	0.15 ± 0.00	0.24 ± 0.03	0.71 ± 0.03***	0.20 ± 0.01	1.78 ± 0.19***
CL (L/h/kg)	2.04 ± 0.07	2.08 ± 0.20	0.52 ± 0.04***	0.34 ± 0.02***	0.21 ± 0.03***
$AUC_{0-\infty}$ (mg/L*h)	2.46 ± 0.08	2.43 ± 0.25	9.26 ± 0.21***	14.65 ± 0.85***	23.66 ± 2.82***

Each value represented as the mean ± SD ($n = 6$)

$^{*}p < 0.05$, $^{***}p < 0.001$ compared with TXA9 group

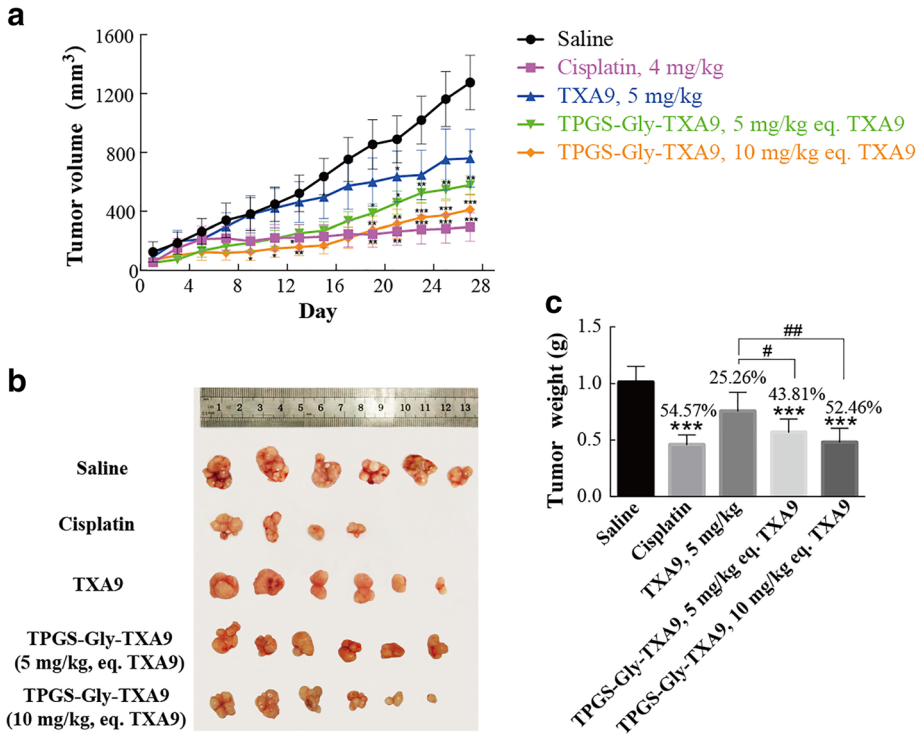

Fig. 6 Antitumor activity of TXA9 (5 mg/kg) and TPGS-Gly-TXA9 (5, 10 mg/kg, eq. TXA9) in A549 xenograft nude mice model (6 mice for each group). Cisplatin group (4 mg/kg) was used as the positive control. (**a**) Tumor volumes of mice during treatment with different drugs. Each value represented as the mean ± SEM (n = 6); (**b**) images of the tumor tissues excised from tumor-bearing nude mice after the treatment with different drugs for 28 days; (**c**) the final tumor weight of mice in each group and the tumor inhibition rates (TIRs) which were calculated and labeled above the column of each group. Each value represented as the mean ± SD (n = 6). $^{*}p < 0.05$, $^{**}p < 0.01$, $^{***}p < 0.001$ compare to saline group; $^{\#}p < 0.05$, $^{\#\#}p < 0.01$ compare to TXA9 group.

values of the characteristic proton signals of carriers and TXA9 in ^{1}H-NMR spectra, which was equal to the mole ratio of them. The idea of using the ratio of absolute integral values to determine drug content of prodrugs was inspired from the reported method, which using the relative intensity ratio of characteristic proton signals in ^{1}H-NMR to calculate the

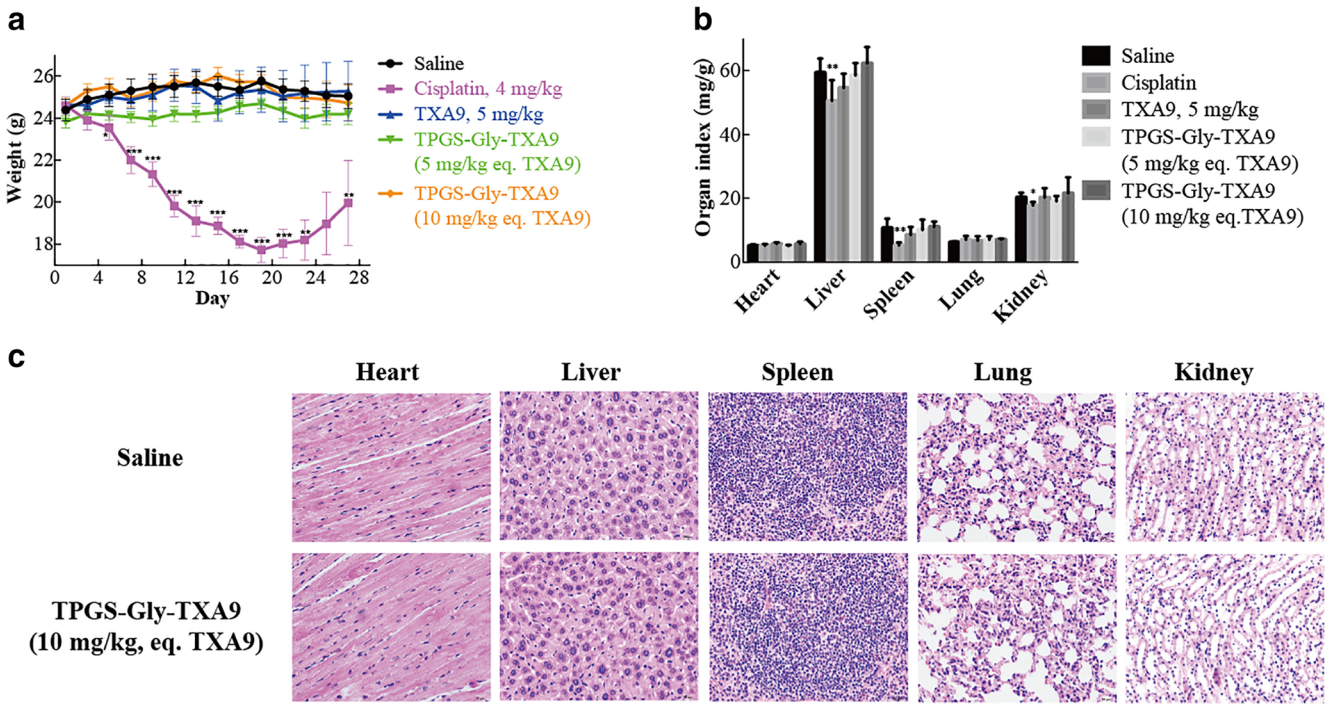

Fig. 7 Systemic toxicity of TPGS-Gly-TXA9 in antitumor activity study *in vivo*. (**a**) The body weight of tumor-bearing nude mice during the treatment of cisplatin, TXA9 and TPGS-Gly-TXA9; (**b**) The organ index of nude mice at the end day after treatment; (C) H&E staining photographs of organ sections (heart, liver, spleen, lung, kidney) after treated by saline and TPGS-Gly-TXA9 (10 mg/kg, equal to TXA9) for 28 days (scale bar: 20 μm). Each value represented as the mean ± SD (n = 6). $^{*}p < 0.05$, $^{**}p < 0.01$, $^{***}p < 0.001$ compare to saline group.

number of repeat units in synthetical polymer (27). By this method, the accurate drug contents of prodrugs were obtained to facilitate the following *in vitro* and *in vivo* experiments.

For the determination of water-solubility, it was found that mPEG prodrugs showed high increasing of water-solubility, which might be attributed to the strong hydrophilicity of mPEG. For TPGS prodrugs, although the hydrophobic structure of α-tocopherol in TPGS limited the ability of PEG to increase water-solubility, the formation of micelles could be an impetus to increase the water-solubility. All prodrugs could improve the water-solubility of TXA9 to reach its therapeutic concentration in water without using any co-solvent.

Due to the amphiphilic structure, TPGS prodrugs could self-assemble to form micelles after dissolved into water. However, mPEG prodrugs failed to form micelles due to the absence of the hydrophobic structure. The CMC values of TPGS-p-TXA9 and TPGS-Gly-TXA9 were 3.47 and 3.23 mg/mL (0.11 and 0.18 mg/mL equal to TXA9), which was higher than that of other TPGS-modified prodrugs (15) due to the poor hydrophobicity of TXA9 and the longer length of PEG chain in TPGS. According to the CMC values, it could be speculated that prodrug micelles would dissociate rapidly along with the dilution of blood after intravenous injection (28). Then the stability of linkage bonds in prodrugs would play an important role in promoting the circulation time of TXA9 *in vivo*.

To estimate the stability of prodrugs, the drug release was measured in pH = 5.0, 7.4, 9.0 PBS and rat plasma respectively. All four prodrugs showed less drug release in pH = 5.0 but more drug release in pH = 7.4 or 9.0, which was attributed to the property of ester bond that it was prone to cleave in the alkaline condition as reported (29). As results shown in Fig. 3, it was found that mPEG-Gly-TXA9 and TPGS-Gly-TXA9 was more prone to release TXA9 than mPEG-p-TXA9 and TPGS-p-TXA9 in acidic environment while showed better stability than other prodrugs in rat plasma (pH = 7.4), indicating that mPEG-Gly-TXA9 and TPGS-Gly-TXA9 could provide better drug release in tumor while remaining stable before entering into tumor tissues. The prolonged plasma circulations of the pristine drug would be the driving force for increased the drug accumulation in tumor tissues and then improved the therapeutic efficacy. To estimate the slow-release effect of prodrugs, pharmacokinetic study *in vivo* was conducted, in which TPGS-Gly-TXA9 exhibited the better pharmacokinetic behavior than the other prodrugs. The potential mechanism of this phenomenon could be attributed to the stability of glycine linker mentioned in stability study *in vitro* and the amphipathic structure of TPGS which might lead to the formation of micelles *in vivo* that could protect TXA9 from escaping the endocytosis of macrophages as reported (30). Besides, the high level of free drug within 10 min after the injection of TPGS-Gly-TXA9 indicated a premature drug release, which might be induced by the rapid distribution into the esterase-rich tissues via the blood circulation *in vivo* and then could accelerate the cleavage of ester bond. However, when compared with the pharmacokinetic behavior of TXA9, the TXA9 released from TPGS-Gly-TXA9 were found with the longer half-life and the greater AUC, indicating that TPGS-Gly-TXA9 could prolong the circulation time of parent drug and therefore increase the drug accumulation in tumor tissues, which might then improve the therapeutic efficacy.

At a cellular level, prodrugs exhibited the desirable cytotoxicity, however, which was a little weaker than that of parent drug. This was properly due to the partial derivatization of hydroxyl group on the C-6' position of sugar in TXA9, and this hydroxyl group might be important to inhibit the growth of cancer cells. For each carrier (mPEG or TPGS), prodrugs with glycine linker had the stronger cytotoxicity than prodrugs with carbonate ester linker, which might be due to the acidic medium induced by the growth of cancer cell during the incubation (31). In this acidic medium, prodrugs with glycine linkers was more prone to release TXA9 than prodrugs with carbonate linkers, which could be confirmed by the *in vitro* stability study at pH = 5.0 PBS. On the other hand, TPGS prodrugs had the lower IC_{50} values than mPEG prodrugs with the same linker. This could be explained that the ester bonds in the remnant TPGS might be gradually cleaved after the release of TXA9, leading to the produce α-TS or α-tocopherol which could enhance the growth-inhibitory effect of chemotherapeutic agents on cancer cells as reported (32–34). What's more, TPGS-Gly-TXA9 exhibited the stronger cytotoxicity than the other three prodrugs, which might be attributed to the synergistic effect between the cleavage of glycine linker and the release of α-TS or α-tocopherol from TPGS.

According to all results above, TPGS-Gly-TXA9 exhibited the most prominent advantages than the other three prodrugs and it was significative to estimate its antitumor activity *in vivo* furthermore. The antitumor activity of TPGS-Gly-TXA9 was further assessed in A549 subcutaneous xenograft nude mice and its antitumor efficacy was significantly stronger than that of TXA9 at the same dose. It could be speculated that the improved pharmacokinetics of TPGS-Gly-TXA9 prolonged the retention time of TXA9 *in vivo*, which may increase the drug accumulation in tumor tissues. Although there was no significant difference between the two dose groups of TPGS-Gly-TXA9 in Fig. 6c, the *p* value of TPGS-Gly-TXA9 low dose group and high dose group were 0.034 and 0.003 respectively when compared with TXA9 group, which showed a trend of increasing significance in tumor inhibition as the dose increased.

CONCLUSION

In this study, four prodrugs were designed and synthesized by conjugating mPEG and TPGS with TXA9 via carbonate ester and glycine linkers, respectively, which aiming to improve the water-solubility, to prolong the circulation time *in vivo* and

to enhance the antitumor efficacy of TXA9. All of four prodrugs could increase the water-solubility of TXA9 dramatically. TPGS-Gly-TXA9 was found with the best stability *in vitro* and the longest half-life *in vivo* among four prodrugs. Then the improved antitumor efficacy of TPGS-Gly-TXA9 was confirmed on A549 xenograft nude mice compared with that of TXA9. Although this study had certified the potential antitumor efficacy of TPGS-Gly-TXA9, the antitumor mechanism should be investigated in further research to provide more evidence for clinical application.

ACKNOWLEDGMENTS AND DISCLOSURES. This research did not receive any specific grant from funding agencies in the public, commercial, or not-for-profit sectors. The authors state no conflict of interest.

REFERENCES

1. Stewart BW, Wild CP. World Cancer report. International Agency for Research on Cancer 2014.
2. Oser MG, Niederst MJ, Sequist LV, Engelman JA. Transformation from non-small-cell lung cancer to small-cell lung cancer: molecular drivers and cells of origin. Lancet Oncol. 2015;16(4):e165–72.
3. Xue R, Han N, Xia MY, Ye C, Hao ZH, Wang LH, *et al.* TXA9, a cardiac glycoside from Streptocaulon juventas , exerts a potent antitumor activity against human non-small cell lung cancer cells in vitro and in vivo. Steroids. 2015;94(23):51–9.
4. Ye C, Wang H, Xue R, Han N, Wang LH, Yang JY, *et al.* Minor cytotoxic cardenolide glycosides from the root of Streptocaulon juventas. Steroids. 2015;93:39–46.
5. Greenwald RB, Yun HC, Mcguire J, Conover CD. Effective drug delivery by PEGylated drug conjugates. Adv Drug Deliv Rev. 2003;55(2):217–50.
6. Banerjee SS, Aher N, Patil R, Khandare J. Poly(ethylene glycol)-Prodrug conjugates: concept, design, and applications. J Drug Deliv. 2012;2012:1–17.
7. Zhang ZP, Tan SW, Feng SS. Vitamin E TPGS as a molecular biomaterial for drug delivery. Biomaterials. 2012;33(19):4889–906.
8. Greenwald RB, Gilbert CW, Pendri A, Conover CD, Xia J, Martinez A. Drug delivery systems: water soluble taxol 2'-poly(ethylene glycol) ester prodrugs-design and in vivo effectiveness. J Med Chem. 1996;39(2):424–31.
9. Sun HP, Zhang Q, Zhang Z, Tong J, Chu DF, Gu JK. Simultaneous quantitative analysis of Polyethylene Glycol (PEG), PEGylated paclitaxel and paclitaxel in rats by MS/MSALL technique with hybrid quadrupole time-of-flight mass spectrometry. J Pharm Biomed Anal. 2017;145:255–61.
10. Ding Y, Zhang P, Tang XY, Zhang C, Ding S, Ye H, *et al.* PEG prodrug of gambogic acid: amino acid and dipeptide spacer effects. Polymer. 2012;53(8):1694–702.
11. Zhao YJ, Wei W, Su ZG, Ma GH. Poly (ethylene glycol) prodrug for anthracyclines via N-Mannich base linker: design, synthesis and biological evaluation. Int J Pharm. 2009;379(1):90–9.
12. Rowinsky EK, Rizzo J, Ochoa L, Takimoto CH, Forouzesh B, Schwartz G, *et al.* A phase I and pharmacokinetic study of pegylated camptothecin as a 1-hour infusion every 3 weeks in patients with advanced solid malignancies. J Clin Oncol. 2003;21(1):148–57.
13. Liu T, Yuan X, Jia TT, Liu C, Ni ZH, Qin ZL, *et al.* Polymeric prodrug of bufalin for increasing solubility and stability: synthesis and anticancer study in vitro and in vivo. Int J Pharm. 2016;506(1–2):382–93.
14. Cao N, Feng SS. Doxorubicin conjugated to D-alpha-tocopheryl polyethylene glycol 1000 succinate (TPGS): conjugation chemistry, characterization, in vitro and in vivo evaluation. Biomaterials. 2008;29:3856–65.
15. Bao YL, Guo YY, Zhuang XT, Li D, Cheng BL, Tan SW, *et al.* D-α-tocopherol polyethylene glycol succinate-based redox-sensitive paclitaxel prodrug for overcoming multidrug resistance in cancer cells. Mol Pharm. 2014;11(9):3196–209.
16. Anbharasi V, Cao N, Feng SS. Doxorubicin conjugated to D-alpha-tocopheryl polyethylene glycol succinate and folic acid as a prodrug for targeted chemotherapy. J Biomed Mater Res A. 2010;94A(3):730–43.
17. Lu L, Yan Z, Weng S, Zhu W, Qin L. Complete regression of xenograft tumors using biodegradable mPEG-PLA-SN38 block copolymer micelles. J Colloids Surf B Biointerfaces. 2016;142:417–23.
18. Wei Z, Hao J, Yuan S, Li Y, Juan W, Sha X, *et al.* Paclitaxel-loaded Pluronic P123/F127 mixed polymeric micelles: formulation, optimization and in vitro characterization. Int J Pharm. 2009;376(1–2):176–85.
19. Hu X, Liu RL, Zhang D, Zhang J, Li ZH, Luan YX. Rational design of an amphiphilic chlorambucil prodrug realizing self-assembled micelles for efficient anticancer therapy. ACS Biomater Sci Eng. 2018;4:973–980.
20. Lommerse J P M, Price S L, Taylor R. Hydrogen bonding of carbonyl, ether, and ester oxygen atoms with alkanol hydroxyl groups. J Comput Chem. 1997;18(6):757–774.
21. Hao T, Chen D, Liu K, Qi Y, Li Z. Micelles of d-α-tocopheryl polyethylene glycol 2000 succinate (TPGS 2K) for doxorubicin delivery with reversal of multidrug resistance. ACS Appl Mater Interfaces. 2015;7(32):18064–75.
22. Vig BS, Huttunen KM, Laine K, Rautio J. Amino acids as promoieties in prodrug design and development. Adv Drug Deliv Rev. 2013;65(10):1370–85.
23. Pasut G, Veronese FM. Polymer–drug conjugation, recent achievements and general strategies. Prog Polym Sci. 2007;32(8):933–61.
24. Roy HK, DiBaise JK, Black J, Karolski WJ, Ratashak A, Ansari S. Polyethylene glycol induces apoptosis in HT-29 cells: potential mechanism for chemoprevention of colon cancer. FEBS Lett. 2001;496(2–3):143–6.
25. Veronese FM, Schiavon O, Pasut G, Mendichi R, Andersson L, Tsirk A, *et al.* PEG-doxorubicin conjugates:influence of polymer structure on drug release,in vitro cytotoxicity,biodistribution,and antitumor activity. Bioconjug Chem. 2005;16(4):775–84.
26. Lu B, Huang D, Zheng H, Huang ZJ, Xu PH, Xu HX, *et al.* Preparation, characterization, and in vitro efficacy of O-carboxymethyl chitosan conjugate of melphalan. Carbohydr Polym. 2013;98(1):36–42.
27. Sun JJ, Liu YH, Chen YC, Zhao WC, Zhai QY, Rathod S, *et al.* Doxorubicin delivered by a redox-responsive dasatinib-containing polymeric prodrug carrier for combination therapy. J Control Release. 2017;258:43–55.
28. Sun X, Guowei W, Hao Z, Shiqi H, Xin L, Jianbin T, *et al.* The blood clearance kinetics and pathway of polymeric micelles in cancer drug delivery. ACS Nano. 12:6179–92.
29. Li M, Liang Z, Sun X, Gong T, Zhang Z. A polymeric prodrug of 5-fluorouracil-1-acetic acid using a multi-hydroxyl polyethylene glycol derivative as the drug carrier. PLoS One. 2014;9(11):e112888.
30. Luo C, Sun J, Liu D, Sun BJ, Lei M, Musetti S, *et al.* Self-assembled redox dual-responsive prodrug-nanosystem formed by single

thioether-bridged paclitaxel-fatty acid conjugate for cancer chemotherapy. Nano Lett. 2016;16(9):5401–8.
31. Webb BA, Chimenti M, Jacobson MP, Barber DL. Dysregulated pH: a perfect storm for cancer progression. Nat Rev Cancer. 2011;11(9):671–7.
32. Prasad KN, Kumar B, Yan XD, Hanson AJ, Cole WC. α-Tocopheryl succinate, the Most effective form of vitamin E for adjuvant Cancer treatment: a review. J Am Coll Nutr. 2003;22(2):108–17.
33. Shanker M, Gopalan B, Patel S, Bocangel D, Chada S, Ramesh R. Vitamin E succinate in combination with mda-7 results in enhanced human ovarian tumor cell killing through modulation of extrinsic and intrinsic apoptotic pathways. Cancer Lett. 2007;254:217–26.
34. Pathak AK, Singh N, Khanna N, Reddy VG, Prasad KN, Kochupillai V. Potentiation of the effect of paclitaxel and carboplatin by antioxidant mixture on human lung Cancer H520 cells. J Am Coll Nutr. 2002;21(5):416–21.